Proceeding International Conference on Religion, Science and Education (2026) **5**, 1469-1480

Batik Motif of Mathematical Modeling of Dengue Fever Transmission with the Social Awareness Factor

Faqih Ainul Mubarok, Muhammad Abizart, Muhammad Ali Syafaat, Sugiyanto*
Mathematics Department, Universitas Islam Negeri Sunan Kalijaga, Yogyakarta, Indonesia.

Corresponding author*
sugiyanto@uin-suka.ac.id

Abstract: Dengue Hemorrhagic Fever (DHF) remains one of the major public health problems in tropical regions, including Indonesia. The transmission rate of this disease is strongly influenced by various factors, particularly the level of social awareness within the community toward prevention and control efforts. This study formulates a mathematical model of DHF transmission by incorporating the social awareness factor as an additional compartment. The analysis involves determining the equilibrium points and the basic reproduction number (R_0), as well as testing the stability of the system using the Routh–Hurwitz criteria. The results show two types of equilibrium points, namely the disease-free point (T_1) and the endemic point (T_2). The point T_1 is locally stable when $R_0<1$ and becomes unstable when $R_0>1$, while point T_2 is locally stable if $R_0>1$. Sensitivity analysis indicates that the social awareness parameter has a significant influence on the value of R_0. Furthermore, numerical simulations demonstrate that an increase in social awareness can effectively suppress disease transmission and lead the system toward a disease-free condition. These findings highlight the importance of enhancing public awareness as a key component of sustainable dengue control strategies.

Keywords: Dengue Hemorrhagic Fever, Social Awareness, Mathematical Model, Epidemiological Simulation.

Introduction

Dengue Hemorrhagic Fever (DHF) is one of the infectious diseases caused by the dengue virus transmitted through the bites of *Aedes aegypti* (the primary vector) and *Aedes albopictus* (the secondary vector). This virus belongs to the *Flaviviridae* family and the *Flavivirus* genus, with four antigenic serotypes known as DENV-1, DENV-2, DENV-3, and DENV-4 (Gubler, 1998). Infection by this virus can affect individuals with low immunity, both children and adults, and generally manifests with symptoms such as high fever, muscle and joint pain, and reddish skin rashes. These symptoms usually last for two to seven days during the initial febrile phase, followed by a critical phase occurring within three to seven days afterward. During this phase, symptoms such as abdominal pain, vomiting, difficulty breathing, and plasma leakage may appear, which can lead to death if not treated promptly and properly (Sahu, 2024).

In Indonesia, DHF cases were first reported in Surabaya in 1968, with 58 cases and 24 deaths. Since then, the incidence of DHF has continued to increase significantly every year. According to data from the Ministry of Health, in 2021 there were 73,518 cases with 705 deaths, which sharply increased in 2022 to 143,266 cases with 1,237 deaths. Meanwhile, in 2023, 114,720 cases with 894 deaths were reported, and up to the 43rd week of 2024, 210,644 cases with 1,293 deaths had been recorded across all districts and cities in Indonesia. This trend indicates that the incidence and mortality rates of DHF remain high and tend to increase from year to year (Hendrati, 2023).

The government has made various efforts to reduce the rising number of DHF cases, both through promotive and preventive programs such as *Pemberantasan Sarang Nyamuk* (PSN, Mosquito Nest Eradication) with the 3M Plus movement (draining, covering, reusing waste materials, and using personal protection), as well as curative and rehabilitative measures for patients (N. Aina

ISSN 2829-3355 | EISSN 2828-8467

Rahmania, 2018). Nevertheless, the continuing increase in cases indicates the need for stronger analytical and predictive approaches to support more effective DHF control policies. One such approach is the use of mathematical epidemiological models to analyze the dynamics of disease transmission.

Mathematical models have long been used in epidemiology to explain the mechanisms of infectious disease transmission such as cholera, COVID-19, and DHF [7–10]. This approach allows for quantitative analysis of the factors influencing disease spread while predicting the effects of various control strategies. The commonly used model is the SEIR-based model (Susceptible, Exposed, Infected, Recovered), which divides the population into several compartments according to infection status and interactions. Through this model, stability analysis, equilibrium point determination, and calculation of the basic reproduction number (R_0) can be performed, which serves as an indicator of the potential for disease transmission (R. Resmawan, 2021).

However, most classical DHF models still focus on biological and environmental factors, such as mosquito biting rates, vector mortality rates, and climate effects. In fact, the social awareness of the community also has a significant influence on disease transmission dynamics. Awareness to maintain environmental cleanliness, carry out PSN regularly, and implement individual preventive actions are crucial aspects in breaking the chain of dengue virus transmission. High social awareness can reduce the contact rate between humans and vectors, thereby lowering the R_0 value and slowing disease transmission. Conversely, low public awareness can accelerate case growth, especially in densely populated areas with poor sanitation (D. Aldila, 2023).

Several studies have attempted to incorporate human behavioral factors into DHF transmission models. Dayap and Rabajante (2025) demonstrated that changes in community behavior toward infection levels can be dynamically modeled through an adaptive social awareness function. Handayani et al. (2024) introduced an individual protection factor into the dengue transmission model and found that increased public awareness significantly reduces the infection peak. Meanwhile, Rahman et al. (2024) expanded the model with a non-standard infection rate that reflects variations in community behavior toward infection risks. Nevertheless, there is still a need for a model that explicitly integrates social awareness as a dynamic variable in the system of differential equations to better represent the real impact of awareness changes on disease spread.

Therefore, this study aims to develop a mathematical model of DHF transmission incorporating the social awareness factor, taking into account the interactions between the human population and the vector within the context of adaptive community behavior. The model will be analyzed mathematically to determine equilibrium points, calculate the basic reproduction number (R_0), and perform numerical simulations to assess the effect of increasing social awareness on disease transmission dynamics. Through this approach, it is expected to provide a more comprehensive understanding of the role of social awareness in reducing the transmission rate of DHF, as well as offer a scientific basis for formulating community-based public health policies.

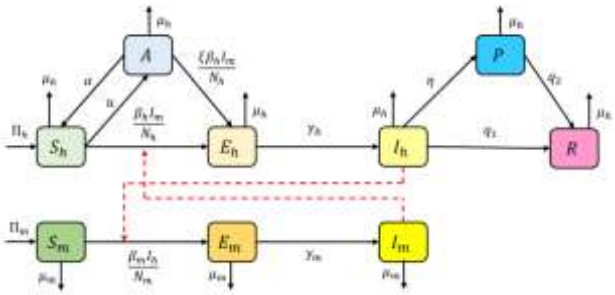

Figure 1. Compartment Diagram of the Mathematical Model of Dengue Fever Transmission

Mathematical Model

The human population is divided into six classes: S_h (individuals susceptible to infection), A (individuals aware of dengue infection), E_h (individuals exposed to the virus), I_h (infected individuals), P (individuals under treatment or hospitalization), and R (individuals recovered from infection). In addition, the mosquito population, as the vector, is divided into three classes: S_m

(susceptible mosquitoes), E_m (exposed mosquitoes, those carrying the virus but not yet infectious), and I_m (infectious mosquitoes capable of transmitting the virus to humans). The transmission diagram illustrating the interaction among each compartment is presented in Figure 1.

Based on the compartment diagram in Figure 1, the mathematical model is formulated as a system of differential equations as follows:

$$\begin{aligned}
\frac{dS_h}{dt} &= II_h - \beta_h \frac{S_h}{N_h} I_m - (u + \mu_h) S_h + \alpha A, \\
\frac{dA}{dt} &= uS_h - (\alpha + \mu_h) A - \xi \beta_h \frac{A}{N_h} I_m, \\
\frac{dE_h}{dt} &= \beta_h I_m \frac{\xi A + S_h}{N_h} - (\gamma_h + \mu_h) E_h, \\
\frac{dI_h}{dt} &= \gamma_h E_h - (q_1 + \eta + \delta + \mu_h) I_h, \\
\frac{dP}{dt} &= \eta I_h - (q_2 + \delta + \mu_h) P, \\
\frac{dR}{dt} &= q_1 I_h + q_2 P - \mu_h R, \\
\frac{S_m}{dt} &= II_m - \beta_m S_m \frac{I_h}{N_m} - \mu_m S_m, \\
\frac{E_m}{dt} &= \beta_m S_m \frac{I_h}{N_m} - (\gamma_m + \mu_m) E_m, \\
\frac{dI_m}{dt} &= \gamma_m E_m - \mu_m I_m.
\end{aligned} \tag{1}$$

The parameters used can be seen in Table 1.

Table 1. Model Parameters.

Parameters	Description
II_h	Birth rate of individuals.
II_m	Birth rate of mosquitoes.
u	Rate of social awareness in preventing the spread of dengue fever.
α	Rate of decline in social awareness.
β_h	Exposure rate of the human population.
β_m	Exposure rate of the mosquito population.
ξ	Effectiveness of infection reduction due to awareness.
γ_h	Extrinsic incubation period in humans.
γ_m	Extrinsic incubation period in mosquitoes.
η	Treatment rate of infected individuals.
q_1	Natural recovery rate of infected individuals.
q_2	Recovery rate of individuals receiving treatment.
δ	Disease-induced mortality rate.
μ_h	Natural mortality rate of humans.
μ_m	Natural mortality rate of mosquitoes.

Results And Discussion

This section presents the results of the analysis of the mathematical model used to describe the dynamics of disease transmission. The analysis includes determining the model's solution region, identifying equilibrium points, calculating the basic reproduction number (R_0), performing sensitivity analysis, and conducting numerical simulations.

Model Solution Region

Lemma 1. The set $\Omega = \{S_h, A, E_h, I_h, P, R, S_m, E_m, I_m\} \in \Re_+^9 : 0 \le N_h \le \frac{II_h}{\mu_h}$ dan $0 \le N_m \le \frac{II_m}{\mu_m}$ is the nonnegative solution region of Eq. (1) represents the total human population, and $N_m$represents the total mosquito population.

Proof. Since $N_h$represents the total human population, then

$$\begin{aligned}
\frac{dN_h}{dt} &= \frac{dS_h}{dt} + \frac{dA}{dt} + \frac{dE_h}{dt} + \frac{dI_h}{dt} + \frac{dP}{dt} + \frac{dR}{dt} \\
&= II_h - \mu_h - \delta(I_h + P).
\end{aligned} \tag{2}$$

Because $I_h + P > 0$, then based on Eq. (2), an inequality is obtained as follows $\frac{dN_h}{dt} \le II_h - \mu_h N_h$. This inequality is then solved using the integrating factor method, yielding:

$$\begin{aligned}
N_h &\le \frac{II_h}{\mu_h}(1 - e^{-\mu_h t}) + N_h e^{\mu_h t} - \\
&\frac{C_1}{\mu_h}(1 - e^{-\mu_h t}).
\end{aligned} \tag{3}$$

Since $\lim_{t \to 0} e^{-\mu_h t} = 1$ and $\lim_{t \to \infty} e^{\mu_h t} = 0$, then based on inequality (3), it follows that $N_h \le \frac{II_h}{\mu_h}$. Because $S_h(t),\ A(t), E_h(t), I_h(t), P(t), R(t)$ are nonnegative, for $T \ge 0$ it follows that $0 \le S_h + A + E_h + I_h + P + R + \frac{II_h}{\mu_h}$.

Similarly, for the mosquito population, we obtain

$$\frac{dN_m}{dt} + \mu_m N_m = \Pi_m. \tag{4}$$

The solution of Eq. (4) is

$$N_m = \frac{II_m}{\mu_m} + \left(N_{m_0} - \frac{II_m}{\mu_m}\right) e^{-\mu_h t}. \tag{5}$$

Since N_m is nonnegative, $\lim_{t\to 0} e^{-\mu_h t} = 1$ and $\lim_{t\to\infty} e^{\mu_h t} = 0$, then based on Eq. (5), we obtain $0 \leq N_m \leq \frac{II_m}{\mu_m}$.

Equilibrium Points and Basic Reproduction Number

The equilibrium points of the model are obtained by assuming that the system is in a constant state, meaning all derivatives of the variables with respect to time are equal to zero. This condition can be expressed as follows:

$$\frac{dS_h}{dt} = \frac{dE_h}{dt} = \frac{dA}{dt} = \frac{dI_h}{dt} = \frac{dP}{dt} = \frac{dR}{dt} = \frac{dS_m}{dt} = \frac{dE_m}{dt} = \frac{dI_m}{dt} = 0\,. \tag{6}$$

Based on Eqs. (1) and (6), two equilibrium points are obtained, namely:

1. **Disease-Free Equilibrium Point** (T_1), which represents the condition when no individuals are infected in either the human or mosquito population. This point is expressed as follows:

$$T_1(S_h, A, E_h, I_h, P, R, S_m, E_m, I_m) = \left(\frac{\alpha A + II_h}{u + \mu_h}, \frac{uS_h}{\alpha + \mu_h}, 0,0,0,0, \frac{II_m}{\mu_m}, 0,0\right).$$

2. **Endemic Equilibrium Point** (T_2), which **represents** the condition when the disease persists and continues to exist within the population. This point is expressed as follows:

$$T_2(S_h, A, E_h, I_h, P, R, S_m, E_m, I_m) = (S_h^*, A^*, E_h^*, I_h^*, P^*, R^*, S_m^*, E_m^*, I_m^*),$$

where

$$S_h^* = \frac{N_h(\alpha A + II_h)}{\beta_h I_m + N_h(u + \mu_h)}$$
$$A^* = \frac{N_h u S_h}{N_h(u + \mu_h) + \xi\beta_h I_m}$$
$$E_h^* = \frac{\beta_h I_m (S_h + \xi A)}{N_h(\gamma_h + \mu_h)}$$
$$I_h^* = \frac{\gamma_h E_h}{q_1 + \eta + \delta + \mu_h}$$
$$P^* = \frac{\eta I_h}{q_2 + \delta + \mu_h}$$
$$R^* = \frac{q_1 I_h + q_2 P}{\mu_h}$$
$$S_m^* = \frac{N_m II_m}{\beta_m I_h + N_m \mu_m}$$
$$E_m^* = \frac{\beta_m I_h S_m}{N_m(\gamma_m + \mu_m)}$$
$$I_m^* = \frac{\gamma_m E_m}{\mu_m}$$

In the analysis of disease-spread dynamics, the basic reproduction number plays an important role as the threshold indicator for an epidemic. This value can be computed using the next generation matrix approach. By this method, we obtain the matrices F and V evaluated at the disease-free equilibrium T_1, namely:

$$F = \begin{pmatrix} 0 & 0 & 0 & 0 & \frac{\beta_h(\alpha + \mu_h + u\xi)}{u + \alpha + \mu_h} \\ 0 & 0 & & 0 & 0 & 0 \\ 0 & 0 & & 0 & 0 & 0 \\ 0 & \beta_m & & 0 & 0 & 0 \\ 0 & 0 & & 0 & 0 & 0 \end{pmatrix}$$

and

$$V = \begin{pmatrix} v_{11} & 0 & 0 & 0 & 0 \\ -\gamma_h & v_{22} & 0 & 0 & 0 \\ 0 & -\eta & v_{33} & 0 & 0 \\ 0 & 0 & 0 & v_{44} & 0 \\ 0 & 0 & 0 & -\gamma_m & \mu_m \end{pmatrix}$$

where

$$v_{11} = \gamma_h + \mu_h, \qquad v_{22} = q_1 + \eta + \delta + \mu_h$$
$$v_{22} = q_2 + \delta + \mu_h, \qquad v_{44} = \gamma_m + \mu_m$$

The basic reproduction number $R_0$is obtained as the dominant eigenvalue, i.e., the largest positive eigenvalue of the matrix $K = FV^{-1}$:

$$K = \begin{pmatrix} 0 & 0 & 0 & k_{13} & k_{14} \\ 0 & 0 & 0 & 0 & 0 \\ 0 & 0 & 0 & 0 & 0 \\ k_{41} & k_{42} & 0 & 0 & 0 \\ 0 & 0 & 0 & 0 & 0 \end{pmatrix}$$

where

$$k_{13} = \frac{\beta_h \gamma_m (\alpha + \mu_h + u\xi)}{(u + \alpha + \mu_h)\mu_m(\gamma_m + \mu_m)} \ , k_{14} = \frac{\beta_h(\alpha + \mu_h + u\xi)}{(u + \alpha + \mu_h)\mu_m}$$

$$k_{41} = \frac{\beta_m \gamma_h}{(\gamma_h + \mu_h)(q_1 + \delta + \eta + \mu_h)} \ , k_{42} = \frac{\beta_m}{q_1 + \delta + \eta + \mu_h}$$

Because $R_0 = \rho(FV^{-1})$, we obtain

$$R_0 = \sqrt{\frac{\beta_h \, \beta_m \gamma_h \gamma_m (\alpha + \mu_h + u\xi)}{(u + \alpha + \mu_h)(q_1 + \delta + \eta + \mu_h)(\gamma_h + \mu_h)\mu_m(\gamma_m + \mu_m)}}$$

Suppose $R_1 = R_0^2$ is obtain as

$$R_1 = \sqrt{\frac{\beta_h \, \beta_m \gamma_h \gamma_m (\alpha + \mu_h + u\xi)}{(u + \alpha + \mu_h)(q_1 + \delta + \eta + \mu_h)(\gamma_h + \mu_h)\mu_m(\gamma_m + \mu_m)}}$$

Next, the value R_1 is used as a reference in the proofs of Theorem 1 and Theorem 2.

Stability Analysis of Equilibrium Points

Stability analysis of equilibrium points is an important aspect in understanding the behavior of disease-spread dynamics in a system. To assess that stability, we evaluate the eigenvalues of the Jacobian matrix obtained by linearizing the dynamical system around the equilibrium point.

Theorem 1. The disease-free equilibrium point T_1 is locally asymptotically stable if $R_0 < 1$and becomes unstable if $R_0 > 1$.

Proof. The Jacobian matrix evaluated at the disease-free equilibrium T_1 for system (1) is given as follows:

$$J_{T_1} = \begin{pmatrix} Z_{11} & \alpha & 0 & 0 & 0 & 0 & 0 & 0 & 0 & Z_{19} \\ u & Z_{22} & 0 & 0 & 0 & 0 & 0 & 0 & 0 & Z_{29} \\ 0 & 0 & Z_{33} & 0 & 0 & 0 & 0 & 0 & 0 & Z_{39} \\ 0 & 0 & 0 & \gamma_h & Z_{44} & 0 & 0 & 0 & 0 & 0 \\ 0 & 0 & 0 & 0 & \eta & Z_{55} & 0 & 0 & 0 & 0 \\ 0 & 0 & 0 & 0 & q_1 & q_2 & Z_{66} & 0 & 0 & 0 \\ 0 & 0 & 0 & 0 & Z_{74} & 0 & 0 & Z_{77} & 0 & 0 \\ 0 & 0 & 0 & 0 & \beta_m & 0 & 0 & 0 & Z_{88} & 0 \\ 0 & 0 & 0 & 0 & 0 & 0 & 0 & 0 & \gamma_m & Z_{99} \end{pmatrix}$$

where

$$Z_{11} = -u - \mu_h \ , Z_{19} = -\frac{\beta_h(\alpha + \mu_h)}{u + \alpha + \mu_h} \ , Z_{22} = -\alpha - \mu_h$$

$$Z_{29} = -\frac{\beta_h u\xi}{u + \alpha + \mu_h} \ , Z_{33} = -\gamma_h - \mu_h \ , Z_{39} = \frac{\beta_h(\alpha + \mu_h + u\xi)}{(u + \alpha + \mu_h)}$$

$$Z_{44} = -\, q_1 - \delta - \eta - \mu_h \ , Z_{55} = -\, q_2 - \delta - \mu_h \ , Z_{66} = -\mu_h \ , Z_{74} = -\, \beta_m$$

$$Z_{77} = -\mu_m \ , Z_{88} = -\gamma_m - \mu_m \ , Z_{99} = -\mu_m$$

The eigenvalues of the matrix $J(T_1)$ can be determined by solving the following characteristic equation:

$$\det\left(J_{T_1} - \lambda I\right) = 0 \qquad (7)$$

Based on Eq. (7) we obtain

$$\lambda_1 = \lambda_2 = -\mu_h$$
$$\lambda_3 = -\mu_m$$
$$\lambda_4 = -u - \alpha - \mu_h$$
$$\lambda_5 = -\, q_2 - \delta - \mu_h$$

and

$$\lambda_4 + a_1\lambda^3 + a_2\lambda^2 + a_3\lambda + a_2 = 0 \qquad (8)$$

where

$$a_1 = q_1 + \delta + \eta + \gamma_h + \gamma_m + 2(\mu_h + \mu_m)$$

$$a_2 = \gamma_m\delta + \gamma_m\eta + 2\gamma_m\mu_h + \eta\mu_h + \delta\mu_h + \mu_h^2 + \left(\gamma_m + 2(\delta + \eta + 2\mu_h)\right)\mu_m + \mu_m^2 + q_1(\gamma_m + \gamma_h + \mu_h + 2\mu_m) + \gamma_h(\gamma_m + \delta + \eta + 2\mu_m + \mu_h)$$

$$a_3 = \gamma_m(\gamma_h + \mu_h)(q_1 + \delta + \eta + \mu_h) + \Big(\gamma_m(\delta + \eta) + 2\mu_h^2 + 2(\gamma_m + \delta + \eta)\mu_h + q_1(\gamma_m + 2\gamma_h + 2\mu_h) + \gamma_h\left(\gamma_m + 2(\delta + \eta + \mu_h)\right)\Big)\mu_m + (q_1 + \delta + \eta + 2\mu_h + \gamma_h)\mu_m^2$$

$$a_4 = (1 - R_1)(q_1 + \delta + \eta + \mu_h)(\gamma_h + \mu_h)\mu_m(\gamma_m + \mu_m)$$

Since all parameters are positive, it follows that $\lambda_i < 0$ for each $i = 1,2,3,4,5$. Meanwhile, the eigenvalues λ_i for $i = 6,7,8,9$ are determined through the analysis of Eq. (8). The coefficients a_i for $i = 1,2,3$ are generally positive. However, the value of a_4 depends on the magnitude of R_0.

If $R_0 < 1$, then $R_1 < 1$, which makes a_4 positive. Furthermore, it can be shown algebraically that $a_1 a_2 a_3 > a_2^3 + a_1^2 a_4$. By applying the Routh–Hurwitz criterion, it can be concluded that the disease-free equilibrium point T_1 is locally asymptotically stable.

Conversely, if $R_0 > 1$, then $R_1 > 1$, which causes $a_4 < 0$. Based on the properties of fourth-degree polynomial roots, this condition yields $\lambda_6\lambda_7\lambda_8\lambda_9 < 0$. This indicates that there exists at least one eigenvalue with a sign different from the others, implying that the disease-free equilibrium point T_1 becomes unstable.

Theorem 2. The endemic equilibrium point $T_2$is locally asymptotically stable if $R_0 > 1$

Proof. Let $\beta_h = \beta_h^*$ be the bifurcation parameter associated with the condition $R_0 = 1$, or equivalently $R_1 = 1$. Through algebraic manipulation, we obtain:

$$\beta_h^* = \frac{(\delta + u + \mu_h)(\gamma_h + \mu_h)(q_1 + \delta + \eta + \mu_h)\mu_m(\gamma_m + \mu_m)}{\beta_m\gamma_m\gamma_h(\alpha + \mu_h + u\xi)}$$

Based on Eq. (8), the condition $R_1 = 1$causes the disease-free equilibrium point $T_1$to have exactly one eigenvalue equal to zero, while the remaining eigenvalues are negative. This zero eigenvalue corresponds to the right eigenvector $(v_1, v_2, v_3, v_4, v_5, v_6, v_7, v_8, v_9)$ and the left eigenvector $(w_1, w_2, w_3, w_4, w_5, w_6, w_7, w_8, w_9)$, which are each given as follows:

$$v_1 = -\frac{(\gamma_h + \mu_h)(q_2 + \delta + \mu_h)(q_1 + \delta + \eta + \mu_h)v_1^*}{\gamma_h(u + \alpha + \mu_h)\big(q_2\eta + q_1(q_2 + \delta + \mu_h)\big)v^{**}}$$
$$v_1^* = (\alpha + \mu_h)^2 + u\alpha\xi$$
$$v_2 = -\frac{u(\gamma_h + \mu_h)(q_2 + \delta + \mu_h)(q_1 + \delta + \eta + \mu_h)v_2^*}{\gamma_h(u + \alpha + \mu_h)\big(q_2\eta + q_1(q_2 + \delta + \mu_h)\big)v^{**}}$$
$$v_2^* = \alpha + \mu_h + (u + \mu_h)\xi$$
$$v^{**} = \alpha + \mu_h + u\xi$$
$$v_3 = \frac{\mu_h(q_2 + \delta + \mu_h)(q_1 + \delta + \eta + \mu_h)}{\gamma_h\big(q_2\eta + q_1(q_2 + \delta + \mu_h)\big)}$$
$$v_4 = \frac{\mu_h(q_2 + \delta + \mu_h)}{q_2\eta + q_1(q_2 + \delta + \mu_h)}$$
$$v_5 = \frac{\eta\mu_h}{q_2\eta + q_1(q_2 + \delta + \mu_h)}$$
$$v_6 = 1$$
$$v_7 = -\frac{\beta_m\mu_h(q_2 + \delta + \mu_h)}{\big(q_2\eta + q_1(q_2 + \delta + \mu_h)\big)\mu_m}$$
$$v_8 = \frac{\beta_m\mu_h(q_2 + \delta + \mu_h)}{\big(q_2\eta + q_1(q_2 + \delta + \mu_h)\big)(\mu_m + \gamma_m)}$$
$$v_9 = \frac{\beta_m\mu_h\gamma_m(q_2 + \delta + \mu_h)}{\big(q_2\eta + q_1(q_2 + \delta + \mu_h)\big)\mu_m(\mu_m + \gamma_m)}$$

and

$$w_1 = 0\,, w_2 = 0\,, w_3 = 1$$
$$w_4 = \frac{\mu_h + \gamma_h}{\gamma_h}\,, w_5 = 0\,, w_6 = 0$$
$$w_7 = 0\,, w_8 = \frac{(\mu_h + \gamma_h)(q_1 + \eta + \delta + \mu_h)}{\beta_m\gamma_h}\,, w_9 = \frac{(\mu_h + \gamma_h)(q_1 + \eta + \delta + \mu_h)(\mu_m + \gamma_m)}{\beta_m\gamma_h\gamma_m}$$

Based on the Castillo–Chavez theorem, the bifurcation constants $a$and $b$are calculated as follows:

$$a = \sum_{k=1}^{9}\sum_{i=1}^{9}\sum_{j=1}^{9} v_k w_i w_j \frac{\partial^2 f_k}{\partial x_i \partial x_j}\Big|_{(T_1,\beta_h^*)} \tag{9}$$
$$a = \sum_{k=1}^{9}\sum_{i=1}^{9} v_k w_i \frac{\partial^2 f_k}{\partial x_i \partial \beta_h}\Big|_{(T_1,\beta_h^*)}$$

By defining $x_1 = S_h$, $x_2 = A$, $x_3 = E_h$, $x_4 = I_h$, $x_5 = P$, $x_6 = R$, $x_7 = S_m$, $x_8 = E_m$, and $x_9 = I_m$, the partial derivatives of f_3 and f_8 are obtained as follows:

$$\frac{\partial^2 f_3}{\partial x_1 \partial x_9}(T_1, \beta_h^*) = \frac{\partial^2 f_3}{\partial x_9 \partial x_1}(T_1, \beta_h^*) = \frac{\mu_h\beta_h^*}{II_h}$$
$$\frac{\partial^2 f_3}{\partial x_2 \partial x_9}(T_1, \beta_h^*) = \frac{\partial^2 f_3}{\partial x_9 \partial x_2}(T_1, \beta_h^*) = \frac{\mu_h\beta_h^*\xi}{II_h}$$
$$\frac{\partial^2 f_8}{\partial x_4 \partial x_7}(T_1, \beta_h^*) = \frac{\partial^2 f_8}{\partial x_7 \partial x_4}(T_1, \beta_h^*) = \frac{\mu_m\beta_m}{II_m}$$
$$\frac{\partial^2 f_3}{\partial x_9 \partial \beta_h}(T_1, \beta_h^*) = \frac{\mu_h + \xi + \alpha}{u + \alpha + \mu_h}$$

Based on the substitution into Eq. (9), we obtain:

$$a = -\frac{2\beta_m \mu_h^2 (q_2 + \delta + \mu_h)^2}{\left(q_2\eta + q_1(q_2 + \delta + \mu_h)\right)^2}\left[\frac{a^*}{a^{**}}v_3 + \frac{\beta_m}{II_m}v_8\right] < 0$$

$$b = \frac{\beta_m \mu_h \gamma_m (q_2 + \delta + \mu_h)(\alpha + \mu_h + u\xi)}{(\alpha + u + \mu_h)\left(q_2\eta + q_1(q_2 + \delta + \mu_h)\right)\mu_m(\mu_m + \gamma_m)}v_3 > 0$$

where

$$a^* = \beta_h^* \gamma_m (\mu_h + \gamma_h)(q_1 + \eta + \delta + \mu_h)\left((\alpha + \mu_h)^2 + u\alpha\xi(\alpha + \mu_h + (u + \mu_h)\xi)\right)$$

$$a^{**} = \gamma_h (u + \alpha + \mu_h)\mu_m(\mu_m + \gamma_m)(\alpha + \mu_h + u\xi)II_h$$

According to the Castillo–Chavez theorem, the conditions $a < 0$and $b > 0$indicate that system (1) undergoes a forward bifurcation when $R_0 = 1$. Thus, as the value of R_0 increases beyond the threshold of one, the disease-free equilibrium point T_1 changes from stable to unstable, whereas the equilibrium point T_2 shifts from unstable to locally asymptotically stable.

Simulation

The simulation was carried out using MATLAB to illustrate the behavior of the model solution over time based on the predetermined parameter values. Some parameter values were obtained from secondary data sourced from various references, while the rest were determined based on assumptions consistent with the context of the model. The initial parameter values used are presented in Table 2.

Table 2. Model Parameter Values.

Parameter	Nilai	Parameter	Nilai
II_h	$\frac{10.560.000}{71{,}35 * 365}$	γ_m	0,7186
II_m	3.839,9	η	0,055
u	0,028	q_1	$\frac{1}{14}$
α	0,004	q_2	0,234
β_h	0,14133	δ	0,0969
β_m	0,048	μ_h	$\frac{1}{71{,}35 * 365}$
ξ	$1{,}17 * 10^{-6}$	μ_m	$\frac{2}{21^2}$
γ_h	0,555		

Graph Interpretation

1. Graph of S_h (Susceptible) – $R^0 < 1$

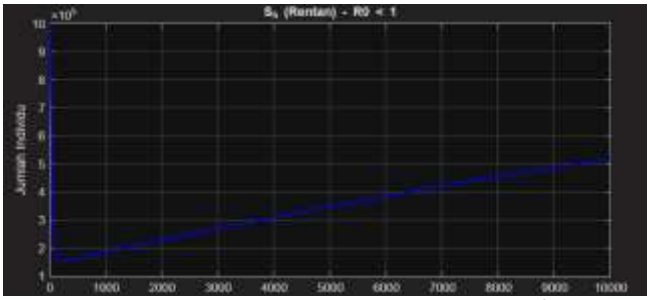

Figure 2. Dynamics of the S_h(Susceptible) Population – $R^0 < 1$

Based on the simulation results for the S_h (susceptible) graph, it can be seen that the number of susceptible individuals decreases at the beginning of the observation period, indicating the occurrence of disease transmission in the early phase of population dynamics. However, over time, the number of susceptible individuals gradually increases until it reaches stability. This pattern illustrates that under the condition $R_0 < 1$, the rate of disease transmission is below the epidemic threshold, so the infection cannot sustain its spread within the population. As a result, the susceptible population increases again as infection cases decrease and new individuals possibly enter the population. Thus, these results show that the disease cannot spread continuously when R_0 is below one.

2. Graph of A (Aware) – $R^0 < 1$

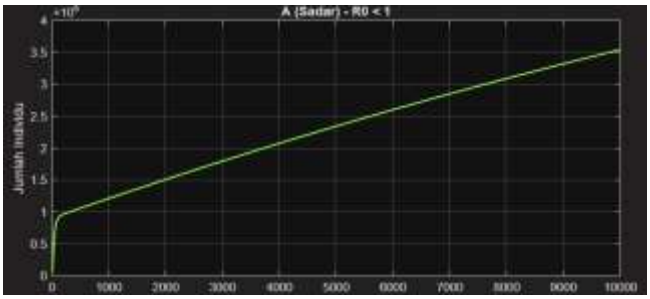

Figure 3. Dynamics of the A(Aware) Population – $R^0 < 1$

The A(aware) graph shows a consistent increase in the number of aware individuals over time. This indicates that public awareness regarding disease prevention and control efforts increases significantly during the simulation period. This

increase contributes to reducing the transmission rate, as aware individuals tend to adopt preventive behaviors such as maintaining environmental hygiene, avoiding vector bites, and actively participating in public health activities. Therefore, the rise in the number of aware individuals plays an important role in keeping R_0 below one and serves as a key factor in suppressing disease spread.

3. Graph of E_h(Exposed Humans) – $R^0 < 1$

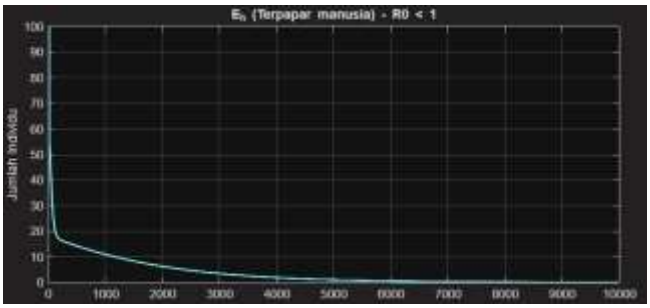

Figure 4. Dynamics of the E_h(Exposed Human) Population – $R^0 < 1$

The simulation results for the E_h (exposed human) graph show a significant decrease in the number of exposed individuals from the beginning of the period until approaching zero at the end of the observation. This phenomenon indicates that disease transmission cannot persist in the human population. The decline in exposed individuals reflects the effectiveness of social interventions and increased awareness in reducing the potential for disease exposure. Under the condition $R^0 < 1$, the average number of secondary cases generated by one infected individual is below one, so the transmission chain is broken, and exposure in the population continues to decline.

4. Graph of I_h(Infected Humans) – $R^0 < 1$

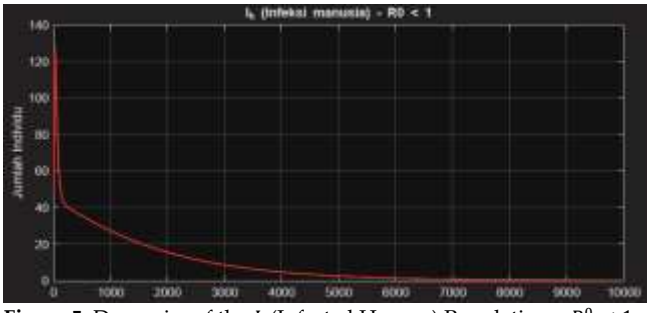

Figure 5. Dynamics of the I_h(Infected Human) Population – $R^0 < 1$

The I_h(infected human) graph shows an exponential decrease in the number of infected individuals over time. At the initial stage, the number of infection cases is relatively high but gradually decreases until approaching zero. This condition indicates that when $R^0 < 1$, the transmission rate is insufficient to sustain infection within the population. The decline also demonstrates the success of disease prevention and control strategies, both through increased public awareness and natural recovery mechanisms. Therefore, the population tends to move toward a disease-free equilibrium, indicating the achievement of zero-endemic stability.

5. Graph of P(Treatment) – $R^0 < 1$

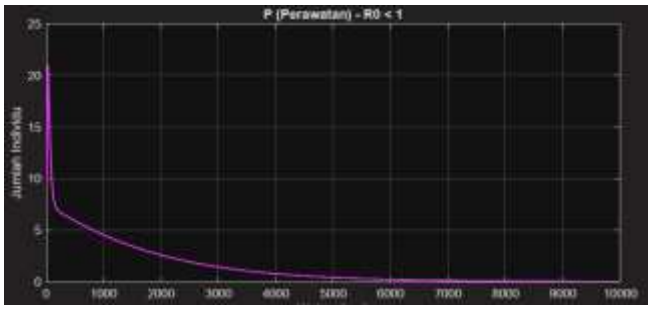

Figure 6. Dynamics of the P(Treatment) Population – $R^0 < 1$

The graph shows the dynamics of the number of individuals under treatment (P) over time under the condition $R^0 < 1$. It is observed that at the beginning of the observation period, the number of treated individuals is relatively high, but over time, it decreases exponentially until approaching zero. This pattern illustrates that when $R^0 < 1$, each infected individual cannot transmit the disease to more than one person, gradually breaking the transmission chain. In epidemiological terms, this condition indicates that the disease is below the epidemic threshold and cannot sustain itself in the population. The decline in the number of treated individuals nearly to zero signifies the success of disease control efforts, both through medical intervention and behavioral changes in society. Hence, this graph emphasizes that maintaining R_0 below one is the key factor in effectively halting the spread of dengue fever.

6. Graph of S_h(Susceptible) – $R^0 > 1$

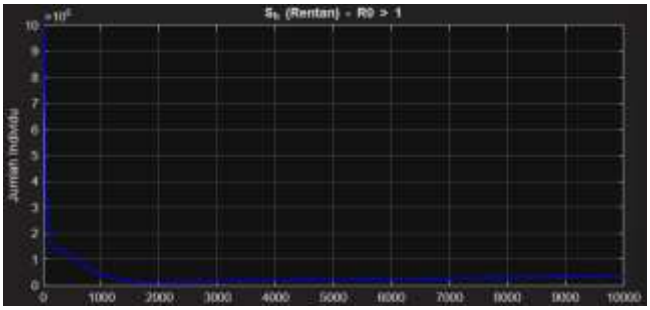

Figure 7. Dynamics of the S_h(Susceptible) Population – $R^0 > 1$

The graph shows that the number of susceptible individuals (S_h) declines sharply in the early phase of the simulation. This decrease reflects the high transmission rate of the disease when $R^0 > 1$, indicating that each infected individual can transmit the disease to more than one person. After the rapid decline, the number of susceptible individuals approaches zero and then stabilizes. This phenomenon indicates that most of the population has been infected or has acquired immunity, suggesting that the disease reaches an endemic state with very low susceptibility levels.

7. Graph of A(Aware) – $R^0 > 1$

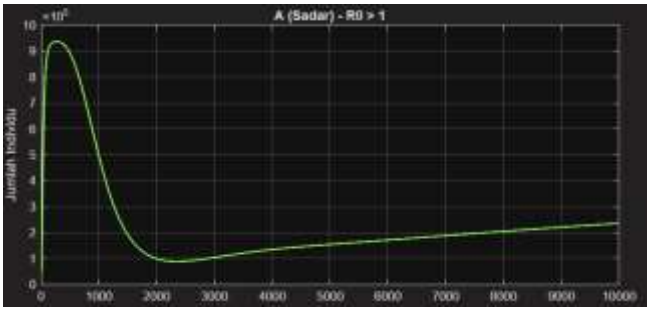

Figure 8. Dynamics of the A(Aware) Population – $R^0 > 1$

The A (aware) graph displays a dynamic pattern, starting with a decrease in awareness during the early period, followed by a gradual long-term increase. The initial decrease reflects the low level of public concern or knowledge about infection risks at the early stage of disease spread. However, after the epidemic's impact becomes widely felt, public awareness rises, which gradually improves the system's condition. The increase in aware individuals in the later period indicates that behavioral interventions and improved awareness contribute to reducing transmission and achieving endemic equilibrium.

8. Graph of E_h(Exposed Humans) – $R^0 > 1$

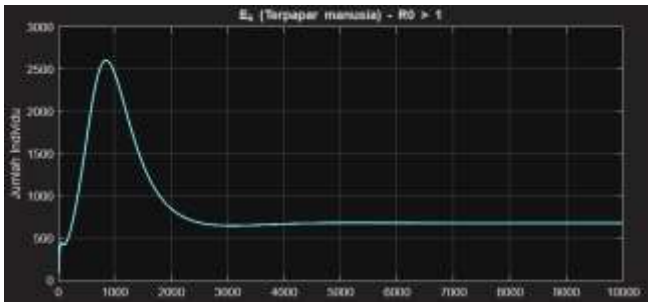

Figure 9. Dynamics of the E_h(Exposed Human) Population – $R^0 > 1$

The E_h (exposed) graph shows a rapid increase reaching its peak around day 1000, followed by a decline toward a stable condition. This peak represents the period of highest transmission intensity, during which infection spreads massively within the population. After the peak phase, the decline in exposed individuals indicates the formation of population immunity, although the number of exposed individuals does not return to zero. This implies that the disease persists at an endemic level, where transmission continues on a limited scale.

9. Graph of I_h(Infected Humans) – $R^0 > 1$

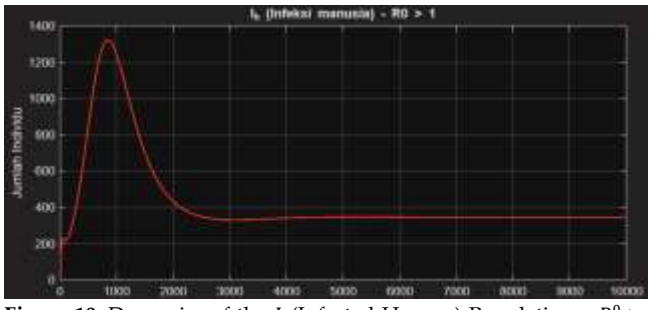

Figure 10. Dynamics of the I_h(Infected Human) Population – $R^0 > 1$

The I_h graph shows that when $R_0 > 1$, the number of infected individuals increases sharply at the beginning of the simulation, peaking around day 800, then decreasing and stabilizing around 350 individuals. This pattern illustrates that in the early phase of the epidemic, disease spread is rapid due to high contact rates between susceptible and infected individuals. However, as a portion of the

population acquires immunity or recovers, the infection rate declines until reaching an endemic equilibrium. This condition indicates that the disease cannot be completely eliminated from the population but persists at a relatively low and stable level in the long term.

10. Graph of P(Treatment) – $R^0 > 1$

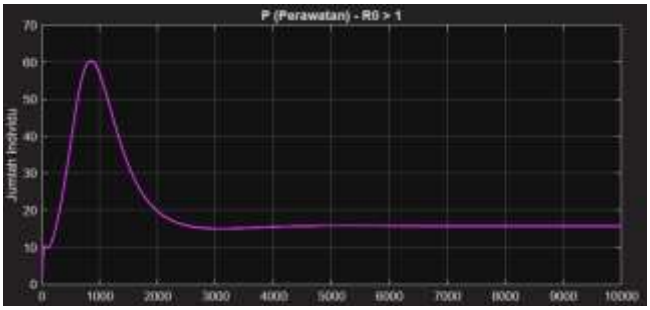

Figure 11. Dynamics of the P(Treatment) Population – $R^0 > 1$

The Pgraph shows the dynamics of individuals undergoing treatment, which rises sharply at the beginning of the period, peaking around day 800 with a maximum of about 60 individuals, then decreasing and stabilizing around 15 individuals. This pattern aligns with the trend in human infection, where an increase in active cases leads to a surge in treatment demand, followed by a decline as disease spread becomes controlled. The stable number of treated individuals in the final phase indicates that the disease reaches an endemic phase, where infection and treatment rates remain constant over time, even though the disease does not completely disappear from the population.

BATIK

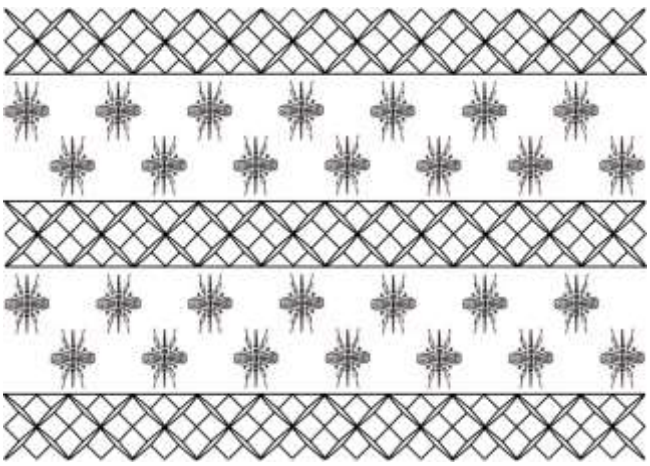

Figure 12. Batik Motif of Dengue Fever Disease Modeling

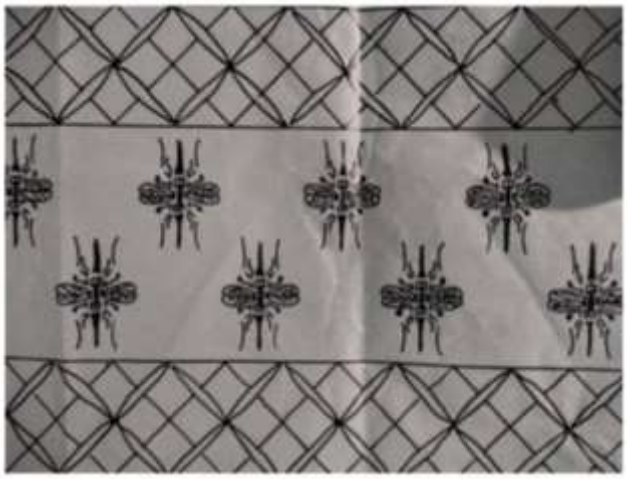

Figure 13. Visualization of Dengue Fever Batik on Tracing Paper

Philosophy of the Batik Motif

This batik motif illustrates a fusion between local wisdom and modern science. Just as the batik-making process requires patience, precision, and repetition, efforts to control dengue hemorrhagic fever (DHF) also demand cooperation and consistency from all parties. Batik thus becomes a medium that unites cultural values with scientific messages.

The repetition of patterns in this design symbolizes continuity and the rhythm of social life. It serves as a reminder that small, repeated actions, such as maintaining cleanliness or covering water containers, can have a significant impact on public health. In this context, batik is not merely an art form but also a reminder that collective habits play a vital role in disease prevention.

The contrast between black and white in the motif carries a meaning of balance. Black symbolizes vigilance against disease threats, while white represents hope and purity. The harmony between these colors reflects the aspiration of a healthy, harmonious society that is aware of the importance of maintaining the environment.

Biological Philosophy

The image of the mosquito at the center serves as the main symbol representing the vector of the Dengue Hemorrhagic Fever (DHF) disease. Its central placement signifies the mosquito's role as a connector between humans, the virus, and the environment. This philosophy emphasizes that the core issue of DHF lies not only in the virus itself but also in understanding the vector's life cycle.

The repetition of the mosquito pattern represents the biological cycle, from egg, larva, and pupa, to adulthood. Each stage plays a crucial role in the mosquito's population sustainability, meaning that disease control must be carried out comprehensively across all stages. The repetition of this pattern symbolizes the continuity of life and the interconnectedness of biological elements.

Mathematical Philosophy

The floral motif formed from the graph $R_0 > 1$ symbolizes the threshold in disease transmission. A value of R_0greater than one represents uncontrolled case growth, depicted through a "blooming flower" as a metaphor for the widespread outbreak. This symbol shows how mathematical data can be transformed into a visual form that is both communicative and meaningful.

Each petal of the flower reflects key parameters in the epidemic model, such as contact rate, transmission probability, and infection duration. Small changes in a single parameter can alter the entire shape of the flower, signifying how sensitive the epidemic system is to minor dynamics within it. From this, the motif teaches the importance of balance between numerical precision and real-world uncertainty.

Moreover, transforming the graph into a floral form affirms that mathematics is not only about rigid calculations but also about patterns and beauty. Through this visualization, the abstract concept of R_0becomes more accessible and easier to understand, allowing scientific knowledge to be appreciated through an aesthetic approach.

Conclusion

This study successfully formulated and analyzed a mathematical model of Dengue Hemorrhagic Fever (DHF) disease transmission by incorporating social awareness as a dynamic variable influencing the disease's transmission rate. Stability analysis shows that the system has two equilibrium points: a disease-free equilibrium and an endemic equilibrium. The disease-free equilibrium is locally stable when $R_0 < 1$, while the endemic equilibrium becomes stable when $R_0 > 1$.

Numerical simulation results show that an increase in the level of social awareness significantly reduces $R_0$and directs the system toward a disease-free condition. The population of aware individuals increases over time, followed by a decrease in exposed, infected, and treated individuals. This demonstrates that public awareness plays a crucial role in breaking the chain of dengue transmission through preventive behavioral changes and active participation in vector control efforts.

Furthermore, integrating social factors into the mathematical model provides a more realistic depiction of dengue dynamics within the community. This model can serve as a foundation for developing public health policies that emphasize education, social participation, and collective behavior in disease control efforts.

The visualization through the developed batik motif also represents an innovative way to connect scientific and cultural aspects. The motif embodies the integration of biology, mathematics, and culture as a reflection of collaborative spirit in addressing public health challenges.

Thus, it can be concluded that enhancing social awareness is an effective and sustainable strategy for controlling dengue transmission. The model developed in this research is expected to serve as a reference for future studies, including the incorporation of environmental factors, government policies, and medical interventions within a more complex system.

Conflict of Interest: The authors declare that there are no conflicts of interest concerning the publication of this article.

References

Clara Anggriani Djuma, N. A. (2025). Model Matematika Penyebaran Penyakit Demam Berdarah Dengue dengan Faktor Kesadaran Sosial : Analisis dan Simulasi. *Jambura Journal of Mathematics*, 196-204.

D. Aldila, M. Z. (2023). Impact of social awareness, case detection, and hospital capacity on dengue eradication in jakarta: A mathematical model approach. *Enginering Journal*, 691-707.

Dayap J. A, R. J. (2025). Mathematical Model of Dengue Transmission Dynamics with Adaptive Human Behavior. Communication in Biomathematical Sciences.

Gubler, D. J. (1998). Dengue and Dengue Hemorrhagic Fever. *Clinical Microbiology Reviews*, 480-496.

Handayani, D. G. (2024). Mathematical Model of Repellent Effect in Dengue Transmission. *Jurnal Ilmu Matematika dan Terapan, 18(2)*.

Hendrati, N. S. (2023). Hubungan Kasus Demam Berdarah Dengue dengan Kepadatan Penduduk di Jawa Timur Tahun 2019-2020. *Media Gizi Kesmas*, 583-588.

N. Aina Rahmania, S. S. (2018). Tindakan Pemberantasan Sarang Nyamuk (PSN) dan 3M-Plus Sebagai Upaya Pengendalian Vektor dalam Pencegahan Penyakit Demam Berdarah Dengue. *Jurnal Agromedicine*, 524-528.

R. Resmawan, A. N. (2021). Analisis Dinamik Model Transmisi COVID-19 dengan Melibatkan Intervensi Karantina. *Jambura Journal of Mathematic*, 66-79.

Rahman, N. S. (2024). Analisis Kemunculan Solusi Periodik dari Model Matematika Penyebaran DBD dengan Laju Infeksi Tidak Standar. *Jurnal Matematika Integratif*.

Sahu, T. c. (2024). An Early Dengue Virus Fever Diagnostic Tool. *International Journal of Scientific Research In Enginering and Management*, 1-5.